

Proteome Changes after Metabolic Engineering to Enhance Aerobic Mineralization of *cis*-1,2-Dichloroethylene

Jintae Lee,[†] Li Cao,[†] Saw Yen Ow,[‡] Martin E. Barrios-Llerena,[‡] Wilfred Chen,[§]
 Thomas K. Wood,[†] and Phillip C. Wright^{*,‡}

Artie McFerrin Department of Chemical Engineering and Department of Biology, 220 Jack E. Brown Building, Texas A & M University, College Station, Texas 77843-3122, Biological & Environmental Systems Group, Department of Chemical and Process Engineering, The University of Sheffield, Sheffield, S1 3JD United Kingdom, and Department of Chemical and Environmental Engineering, University of California, Riverside, California 92521

Received January 10, 2006

Metabolically engineered *Escherichia coli* has previously been used to degrade *cis*-1,2-dichloroethylene (*cis*-DCE). The strains express the six genes of an evolved toluene *ortho*-monooxygenase from *Burkholderia cepacia* G4 (TOM-Green, which formed a reactive epoxide) with either (1) γ -glutamylcysteine synthetase (GSHI^{*}, which forms glutathione) and the glutathione *S*-transferase IsoLR1 from *Rhodococcus* AD45 (which adds glutathione to the reactive *cis*-DCE epoxide) or (2) with an evolved epoxide hydrolase from *Agrobacterium radiobacter* AD1 (EchA F108L/I219L/C248I which converts the reactive *cis*-DCE epoxide to a diol). Here, the impact of this metabolic engineering for bioremediation was assessed by investigating the changes in the proteome through a quantitative shotgun proteomics technique (iTRAQ) by tracking the changes due to the sequential addition of TOM-Green, IsoLR1, and GSHI^{*} and due to adding the evolved EchA versus the wild-type enzyme to TOM-Green. For the TOM-Green/EchA system, 8 proteins out of 268 identified proteins were differentially expressed in the strain expressing EchA F108L/I219L/C248I relative to wild-type EchA (e.g., EchA, protein chain elongation factor EF-Ts, 50S ribosomal subunits L7/L12/L32/L29, cysteine synthase A, glycerophosphodiester phosphodiesterase, iron superoxide dismutase). For the TOM-Green/IsoLR1/GSHI^{*} system, the expression level of 49 proteins was changed out of 364 identified proteins. The induced proteins due to the addition of TOM-Green, IsoLR1, and GSHI^{*} were involved in the oxidative defense mechanism, pyruvate metabolism, and glutathione synthesis (e.g., 30S ribosomal subunit proteins S3 and S16, 50S ribosomal subunit protein L20, alkyl hydroperoxide reductase, lactate dehydrogenase, acetate kinase, cysteine synthase A). Enzymes involved in indole synthesis, fatty acid synthesis, gluconeogenesis, and the tricarboxylic acid cycle were repressed (e.g., tryptophanase, acetyl-CoA carboxylase, phosphoenolpyruvate carboxykinase, malate dehydrogenase). Hence, the metabolic engineering that leads to enhanced aerobic degradation of 1 mM *cis*-DCE (2.4–4-fold more chloride ions released) and reduced toxicity from *cis*-DCE epoxide results in enhanced synthesis of glutathione coupled with an induced stress response as well as repression of fatty acid synthesis, gluconeogenesis, and the tricarboxylic acid cycle.

Keywords: iTRAQ • metabolic engineering • toluene *ortho*-monooxygenase • γ -glutamylcysteine synthetase • glutathione *S*-transferase • *cis*-1,2-dichloroethylene • quantitative proteomics

Introduction

cis-1,2-Dichloroethylene (*cis*-DCE) is a U.S. EPA priority pollutant,¹ and degrading *cis*-DCE aerobically is important, since anaerobic degradation leads to formation of more toxic vinyl chloride, a human carcinogen.² Previously, metabolic engineering was performed in our lab with *Escherichia coli* to detoxify *cis*-DCE using two different metabolic pathways.^{3,4} In both systems (Figure 1), toluene *ortho*-monooxygenase from *Burkholderia cepacia* G4 (TOM) was used to initiate attack of the chlorinated ethene. TOM consists of a 211-kDa hydroxylase

encoded by *tomA1A3A4* with two catalytic oxygen-bridged binuclear iron centers, a 40-kDa NADH-oxidoreductase encoded by *tomA5*, and a 10.4-kDa electron-transfer protein encoded by *tomA2*. TOM-Green has a VI06A mutation in the α -subunit of the hydroxylase and has enhanced activity toward trichloroethylene, 1,1-dichloroethylene, and *trans*-dichloroethylene.⁵

The first detoxification strategy through *cis*-DCE epoxide was constructed by coexpressing TOM-Green with glutathione *S*-transferase (GST, specifically IsoLR1), and a variant of γ -glutamylcysteine synthetase (GSHI^{*}), which allows overexpression of glutathione (GSH) by overcoming feedback inhibition (Figure 1).⁴ The engineered *E. coli* containing TOM-Green, IsoLR1, and GSHI^{*} enhanced mineralization of *cis*-DCE 4-fold compared with the strain with only TOM-Green.⁴

* Corresponding author. Phone: +44 (0)114 222 7577. Fax: +44(0) 114 2227501. E-mail: p.c.wright@sheffield.ac.uk.

[†] Texas A & M University.

[‡] The University of Sheffield.

[§] University of California.

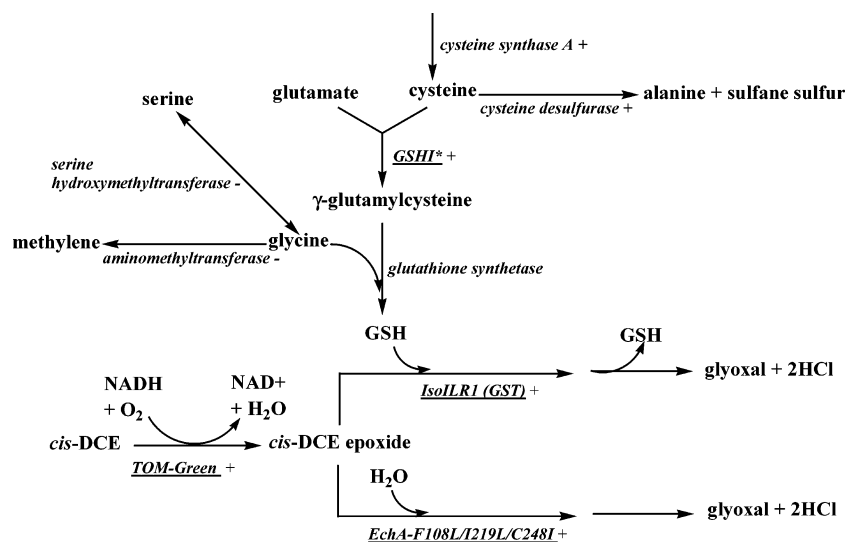


Figure 1. Detoxification pathway for *cis*-DCE by TG1/TOM-Green/*IsoLRL1*/*GSHI** and TG1/TOM-Green/*EchA-F108L/I219L/C248I* (cloned genes are underlined). The “+” indicates overexpression, while “-” indicates repression of the proteins. Two arrows indicate multiple steps. Abbreviations: *cis*-DCE, *cis*-1,2-dichloroethylene; *GSHI**, variant of γ -glutamylcysteine synthetase from *E. coli*; GSH, glutathione; GST, glutathione *S*-transferase; *EchA*, epoxide hydrolase from *A. radiobacter* AD1.

In the second detoxification strategy, GST and *GSHI** were replaced by an epoxide hydrolase, which hydrolyzes reactive epoxides to the corresponding diol. Protein engineering through successive rounds of saturation mutagenesis was required to modify the epoxide hydrolase from *Agrobacterium radiobacter* AD1 (*EchA*, 294 aa) to accept *cis*-DCE epoxide as a substrate (Figure 1).³ When TOM-Green with the F108L/I219L/C248I variant of *EchA* was expressed, 10-fold more *cis*-DCE was mineralized than the strain containing TOM-Green with wild-type *EchA*.³

Recent advances in proteomics have allowed protein expression levels to be determined. A quantitative shotgun approach termed iTRAQ based on reporter ions using tandem mass spectrometry (MS/MS) has been developed.⁶ The approach uses a set of four isobaric reagents that label digested peptides from different samples, and the derivatized peptides in the mixture of samples can be identified and quantified using MS/MS. Hence, this multiplex strategy simultaneously quantifies changes in protein expression level under four different biological conditions.⁶ The technique was successfully used in a proteomic expression analysis of the *rhsA* element, an unknown functional protein related to a transposon in *E. coli*. The study showed that 780 proteins in 17 functional categories could be identified.⁷ Here, we report the proteomic changes in *E. coli* engineered to express 7 to 9 genes for the degradation of *cis*-DCE. The metabolically engineered cells degrade more *cis*-DCE because of enhanced synthesis of glutathione. Although there are other interpretations possible and further work is required to study individual metabolic pathways, the enhanced degradation appears to be a result of induction of a stress response and up-regulation of some ribosomal subunit proteins, as well as repression of fatty acid synthesis, gluconeogenesis, and the tricarboxylic acid cycle.

Materials and Methods

Chemicals, Organisms, and Growth Conditions. All the chemicals were purchased from Fisher Scientific Company (Pittsburgh, PA) except *cis*-DCE (TCI America, Inc., Portland, OR). *E. coli* TG1⁸ were routinely grown at 37 °C in chloride-

free Luria-Bertani (LB) broth supplemented with 100 μ g/mL kanamycin (Kan100), to maintain plasmids based on pBS(Kan), and 50 μ g/mL chloramphenicol (Cam50) for maintaining plasmids pMMB206 or pMMB277. The strains were cultured with initial turbidity at 600 nm of \sim 0.1 from overnight cultures made from fresh single colonies. Isopropyl- β -D-thiogalactopyranoside (IPTG, 0.5 mM) was added to induce the expression of enzymes when the turbidity reached 0.3–0.35. The exponentially grown cells were harvested after induction with IPTG for 2 h, and washed three times with Tris-HNO₃ buffer (50 mM, pH 7.0) at room temperature to remove traces of chloride and metabolic byproducts.⁵

Enzyme Activity and Viability. *cis*-DCE degradation was measured through chloride ion release. The washed cells were adjusted to a turbidity of 2–3.5 with Tris-HNO₃ buffer, and 10 mL of these cells were contacted with 1 mM *cis*-DCE together with 0.5 mM IPTG and 5 mM succinate in 60 mL vials at 37 °C with shaking (250 rpm). Samples (1 mL) were taken periodically for a chloride ion assay using the method of Canada et al.⁵ For the viability test, cells taken from the reaction were serially diluted using Tris-HNO₃ buffer, placed on LB plates containing Kan100 and Cam50, and incubated at 37 °C overnight for colony counting.

Protein Extraction and Quantification. Data reproducibility in technical and biological replicates using the same protein extraction method described by Chong et al.,⁹ and further analysis of that large dataset (C. S. Gan, University of Sheffield, unpublished analysis), reveals that the coefficient of variance (CV) is within a maximal range of 0.1 for iTRAQ labeling experiments in our hands. The information was used as a guideline for protein extraction in *E. coli* here.

After contact with the *cis*-DCE (1 mM) for 2 h, *E. coli* cells (1 mL) were transferred to microcentrifuge tubes, frozen with dry ice and 95% ethanol, and stored at -80 °C. Cells were thawed on ice and centrifuged at 13 000g for 15 min, and the supernatants were discarded. The recovered pellets were resuspended in 500 μ L of TEAB buffer (90 mM triethylammonium bicarbonate, pH 8.6). Prior to cell disruption, the cell suspensions were allowed to incubate at room temperature for 15 min.

Crude protein extracts from each sample were obtained by lysing frozen *E. coli* in liquid nitrogen using a mortar and pestle. Liquid nitrogen was poured into the mortar before pipetting the suspended cells into the mortar. The cells were allowed to freeze and later ground into a fine powder using a cryogenically treated pestle. The grinding was repeated twice prior to recovering the powdered extracts into a clean microcentrifuge tube. The recovered extracts were sonicated for 10 min in an ice-cold water bath and subsequently centrifuged for 30 min at 21 000g. The supernatant containing predominantly soluble proteins was transferred to a new microcentrifuge tube, while the insoluble pellets, which consisted of mostly insoluble proteins, were discarded. The soluble protein concentration was then determined using the RCDC assays (Bio-Rad).

Amine-Modifying Protein Labeling (iTRAQ Labeling). The quantified proteins (100 μ g) from each of the *E. coli* strains were transferred to a new microcentrifuge tube for iTRAQ labeling. The proteins were digested and labeled using the iTRAQ protocol and labeling kit (Applied Biosystems, CA) with some modification. Before running the protocol for the protein digest, a vial of trypsin was reconstituted in 25 μ L of 1mM hydrochloric acid. Aliquots (3 μ L) of reconstituted trypsin solution were added to each sample tube, and another 5 μ L of acetonitrile (ACN) was later added to the respective tubes. During the labeling process, 140 μ L of ethanol was added instead of 70 μ L. Samples were collected after labeling and stored at -20°C prior to HPLC separation.

Cation Exchange Liquid Chromatography (LC). A liquid chromatographic peptide separation was achieved using a PolySULFOETHYL A Packed Column (PolyLC, Columbia, MD) with a 5 μ m particle size and a column dimension of 100 mm \times 2.1 mm i.d., 200 \AA pore size, on a BioLC HPLC unit (Dionex, Surrey, U.K.). The strong cation exchange (SCX) process utilized three separation buffers, A, B, and C. Buffer A had a graduated composition of 10 mM KH_2PO_4 and 25% ACN at pH 2.97; buffer B was composed of 10 mM KH_2PO_4 , 25% ACN, and 500 mM KCl at pH 2.97, while buffer C contained 10 mM KH_2PO_4 , 25% ACN, and 1 M KCl at pH 2.97. The programmed gradients were 100% buffer A for 5 min, linear ramp from 0 to 21% buffer B for 2 min, linear ramp from 21 to 31% buffer B for 3 min, prolonged linear ramp from 31 to 50% B for 25 min, 50–100% buffer B for 10 min, buffer B was dropped to 0%, step increment of 42% buffer C, linear ramp 42–100% buffer C of 5 min, hold 100% buffer C for 5, and 5 min of 100% A. Total separation time was 60 min. The injection volume was 200 μ L, while the flow rate was maintained at 0.2 mL/min. The peptide separation was monitored through a UV Detector UVD170U by the Chromeleon software package version 6.50 (Dionex/LC Packings, The Netherlands). Peptide fractions were then collected at 1 min intervals using a Dionex Foxy Jr. Fraction Collector for 60 min.

LC-MS/MS Analysis. Peptide separation was performed on an Ultimate chromatography system (Dionex-LC Packings, The Netherlands) interfaced to a QSTAR XL (Applied Biosystems-MDS Sciex) tandem mass spectrometer. Individual SCX fractions were injected and captured onto a 0.3×5 mm trap column (3- μ m C18 Dionex-LC Packings) and then eluted onto a 0.075×150 mm analytical column (3- μ m C18 Dionex-LC Packings) using an automated binary gradient (300 mL/min) from 97% buffer A (3% ACN, 0.1% FA) to 45% buffer B (97% ACN, 3% ACN, and 0.1% FA) over 75 min, followed by 90% B for 5 min. Survey scans were acquired from m/z 300–1800 with up to two precursors selected for MS/MS from m/z 65–2000

using dynamic exclusion. The collision energy range was $\sim 20\%$ higher than that used for unlabeled peptides to overcome the stabilizing effect of the basic N-terminal derivative and achieve equivalent fragmentation.

Data Analysis and Interpretation. Peptide and protein identifications were performed using Pro QUANT software v. 1.1 (Applied Biosystems, MDS Sciex) against a modified *E. coli* K-12 protein database (obtained from NCBI, April 2005) with the addition of the TOM-green protein sequences (4250 ORFs) and the EchA peptide (294 aa). The search used a mass tolerance of 0.45 Da for the precursor mass and 0.3 Da for fragment masses, with MMTS as a cysteine fixed modification, and 1 missed cleavage was allowed. A list of protein identifications was generated using ProGroup Viewer v. 1.0.6 (Applied Biosystems, MDS Sciex), for single and multiprotein matches to a protein, with a probability cutoff of 95% to filter matches. ProGroup Viewer v. 1.0.6 is an updated version that fixed many of the software problems in v. 1.0.5. Only protein quantification data with relative expression of >1.8 and <0.6 was chosen to ensure up- and down-regulation authenticity. A guide to false-positive identification was performed by matching the sample iTRAQ-labeled dataset from both systems against a nonrelated bacterium, *Nostoc* sp. PCC7120 (6055 ORFs, NCBI, August 2005), database using Pro QUANT software v. 1.1 (Applied Biosystems, MDS Sciex) at the 95% protein confidence interval. Corresponding peptide identifications above the 70% confidence interval in the *Nostoc* sp. 7120 list were cross-referenced (to remove common peptides) with the peptide identities obtained from the modified *E. coli* (4250 ORFs) database to quantitatively provide a guideline for false-positives identification. Single peptide hits for proteins were not generally used unless they had been manually checked by inspection (examination of coverage of y, a, b, and immonium ions) of spectra and de novo sequencing. Greater confidence for single peptides was given if they had been seen in separate MS experiments (as we performed multiple injections into the MS). The criteria, including the numbers of peptides and times seen, are given in the Supporting Information.

Results

Data Analysis, Proteome Coverage, de Novo Sequencing, and False-Positive Identification. There were 364 proteins identified above 95% protein confidence for the GSHI*/IsoILR1-modified *E. coli* K12 (4250 ORFs) database using Pro QUANT software v. 1.1 (Applied Biosystems, MDS Sciex) based on 4440 peptides. Similarly, a total of 268 positive protein hits were reported in the epoxide hydrolase (EchA) system, which were referenced to 3394 corresponding peptides. The expression ratio, *P*-value, and error factor for proteins identified from both systems were also calculated (Figure 4, and protein list; Supporting Information I and II) (Complete peptide list available upon request.)

There were 111 protein entries in the glutathione *S*-transferase system and 60 proteins in the epoxide hydrolase system that were identified by only one peptide (inclusive of replicates). These peptides identified were checked by ProQuant software v1.1 (Applied Biosystems, MDS Sciex) and were found to not have any immediate association with other proteins within the same proteome.

Only protein quantification data with relative expressions above $+1.8$ and below -0.6 were biologically considered to ensure the leverage of up- and down-regulation that was significant relative to the guideline CV of 0.1 discussed earlier.

Table 1. Cell Viability after 1 mM *cis*-DCE Mineralization by Whole *E. coli* Cells Expressing TOM-Green/EchA F108L/I219L/C248I or TOM-Green/IsoILR1/GSHI*

| | | Viable cells, cells/mL | | | | | |
|---|---------|---|--|---|------------------------------------|------------------------------------|--|
| | | TOM-Green/ EchA wild-type ^a | TOM-Green/EchA F108L/I219L/C248I ^a | pBS(Kan) ⁻ / pMMB277 ^b | TOM-Green/ pMMB277 ^b | TOM-Green/ IsoILR1 ^b | TOM-Green/ IsoILR1/GSHI ^{*b} |
| Time | 0 min | $(1.7 \pm 0.2) \times 10^8$ | $(1.40 \pm 0.08) \times 10^8$ | $(1.49 \pm 0.08) \times 10^8$ | $(1.30 \pm 0.03) \times 10^8$ | $(1.46 \pm 0.17) \times 10^8$ | $(1.96 \pm 0.19) \times 10^8$ |
| | 120 min | $(0.57 \pm 0.06) \times 10^8$ | $(0.42 \pm 0.01) \times 10^8$ | $(1.1 \pm 0.1) \times 10^8$ | $(0.7 \pm 0.3) \times 10^8$ | $(0.72 \pm 0.11) \times 10^8$ | $(1.3 \pm 0.1) \times 10^8$ |
| Viability, % | | 38 ± 6 | 30.5 ± 0.7 | 79 ± 4 | 62 ± 6 | 52 ± 4 | 73 ± 8 |
| Cl ⁻ formation, μM | | 482 | 1017 | 0 | 64 | 179 | 235 |
| Cl ⁻ formation, (mmol/min)/mg protein | | 2.96 | 6.54 | 0 | 0.64 | 1.25 | 2.53 |

^a *E. coli* TG1/pMMB206-TOM-Green/pBS(Kan)-EchA and *E. coli* TG1/pMMB206-TOM-Green/pBS(Kan)-EchA F108L/I219L/C248I. ^b *E. coli* TG1/pBS(Kan)-/pMMB277, *E. coli* TG1/pBS(Kan)-TOM-Green/pMMB277, *E. coli* TG1/pBS(Kan)-TOM-Green/pMMB277-IsoILR1, and *E. coli* TG1/pBS(Kan)-TOM-Green/pMMB277-IsoILR1-GSHI*.

Peptide dataset matching using ProGroup Viewer v. 1.0.6 (Applied Biosystems, MDS Sciex) for false-positive identification also revealed none of the 103 peptide sequences matched in *Nostoc* sp. 7120 were found in the 4440 peptides identified from the *E. coli* protein database for the glutathione *S*-transferase system. This was also true for the false-positive study conducted on the EchA system, as none of the 132 peptides matched in *Nostoc* sp. 7120 were matched with the 3394 peptides in the epoxide hydrolase system. The false-positive identification factor determined was therefore 0.0232 (2.32%) for the glutathione *S*-transferase system and 0.0388 (3.88%) for the epoxide hydrolase system (false-positive identification list; Supporting Information I and II) on this basis.

Four selected proteins identified by a single distinct peptide hit in the glutathione *S*-transferase system (Table 2, and low peptide MS check; Supporting Information) and two from the epoxide hydrolase system (Table 3, and low peptide MS check Supporting Information VI) were manually checked for any misinterpretation of the MS/MS experiments by ProQuant 1.1 (Applied Biosystems, MDS Sciex) on the coverage of γ , a , b , and immonium ions during TOF. Manual checking confirmed satisfactory ion matching for all six identifications (accession numbers: glutathione-*S*-transferase system, 16128171, 16129055, 16130807, and 16131507; epoxide hydrolase system, 16131191 and 16129052). Although the coverage for theoretical γ and b series ions was not complete in two of the six proteins, the abundant presence of less specific fragment immonium ions was sufficient in identifying most if not all of the amino acid fingerprints in the corresponding peptide (ion chromatograms; Supporting Information VI), hence, sufficiently validating their identifications.

The proteome coverage obtained by the 364 proteins obtained using iTRAQ labeling contained more acidic proteins than of comparable basic variants. The total tally of acidic proteins found here accounts for over 75% of the spread across the *E. coli* proteome (Figure 2). Similarly, acidic proteins found in the epoxide hydrolase system also accounts for 75% of the spread across the model proteome.

Mineralization of *cis*-DCE and Cell Viability. We metabolically engineered two systems to degrade *cis*-DCE with both systems relying on initial attack from TOM-Green³ to form a reactive *cis*-DCE epoxide: in the first system, GST (IsoILR1) adds glutathione to the *cis*-DCE epoxide, and in the second system, an engineered epoxide hydrolase (EchA F108L/I219L/C248I) adds water to the *cis*-DCE epoxide (Figure 1). Both adducts are unstable and degrade to release free chloride, so *cis*-DCE is mineralized. Here, 1 mM *cis*-DCE was converted to chloride (Table 1), and these values agree with our previous reports.^{3,4}

To measure cell viability, cells were withdrawn using the same reaction conditions. The number of viable cells decreased after 2 h of degradation of *cis*-DCE for all the strains (Table 1). The introduction of the GST and GSHI* increased cell viability, since the TOM-Green/IsoILR1/GSHI* system had the highest number of viable cells ($73 \pm 8\%$ vs $62 \pm 6\%$ for TOM-Green alone); this increase is more significant than the absolute viability numbers indicate, because the TOM-Green/IsoILR1/GSHI* system generated 4-fold more chloride and toxic intermediates than the TOM-Green system (Table 1). Although there was no significant difference in the number of viable cells after contact with *cis*-DCE between the TOM-Green/wild-type EchA and TOM-Green/EchA F108L/I219L/C248I cultures ($38 \pm 6\%$ vs $30.5 \pm 0.7\%$) (Table 1), if one takes into account that 2.2-fold more chloride as well as 2.2-fold more toxic intermediates, *cis*-DCE epoxide, and glyoxal (Figure 1) were generated in the TOM-Green/EchA F108L/I219L/C248I culture, it is concluded that there was less toxicity with the engineered epoxide hydrolase system, too.

Glutathione *S*-Transferase System Proteome. Samples from all four strains were digested and labeled individually with iTRAQ reagents and analyzed simultaneously by LC-MS/MS. A total of 364 proteins was identified on the basis of single- and multipeptide matches to a protein, with a probability cutoff of 95%. Concentrations of 49 out of the 364 proteins were changed significantly after contact with 1 mM *cis*-DCE in the three strains with TOM-Green compared to the control strain without TOM-Green. Enzymes involved in the detoxification of *cis*-DCE, carbon flux, fatty acid synthesis, and oxidative stress were impacted.

As expected, of the three strains containing TOM-Green, the TOM-Green α subunit (519 aa, encoded by *tomA3*), β subunit (331 aa, encoded by *tomA1*), and γ subunit (118 aa, encoded by *tomA4*) of the hydroxylase were detected along with the NADH-oxidoreductase (354 aa, encoded by *tomA5*); the concentrations of these TOM proteins were 2–9-fold higher concentrations than the control which lacked TOM-Green (Table 2). Also, there was no significant difference in the expression of these subunits in the three strains which expressed TOM-Green, so the remaining effects were the result of metabolic engineering, not TOM-Green expression. Also, as expected, γ -glutamylcysteine synthetase (GSHI*) was identified and found to be present in an 8.6-fold greater concentrations in TG1/TOM-Green/IsoILR1/GSHI* than in the three strains that did not express this enzyme (Figure 1, Table 2).

One result of trying to increase glutathione production by introducing the γ -glutamylcysteine synthetase gene (GSHI*, combines glutamate and cysteine), was that the metabolically engineered cells responded by inducing the machinery required

Table 2. Relative Protein Expression of *E. coli* TG1 Cells Expressing TOM-Green, TOM-Green/IsoILR1, or TOM-Green/IsoILR1/GSHI* Relative to Cells Which Lack These Enzymes

| Protein Name | Peptides > 70% Confidence | | ID number | Gene | Synonym | Ratio ^b | EF Ratio ^b | Ratio ^c | EF Ratio ^c | Ratio ^d | EF Ratio ^d |
|--|---------------------------|----------|----------------|--------------|----------------|--------------------|-----------------------|--------------------|-----------------------|--------------------|-----------------------|
| | Total | Distinct | | | | | | | | | |
| TOM α subunit | 105 | 13 | N ^a | <i>tomA3</i> | N ^a | 8.44 | 1.31 | 4.72 | 1.27 | 8.28 | 1.32 |
| TOM β subunit | 57 | 12 | N ^a | <i>tomA1</i> | N ^a | 5.52 | 1.28 | 6.99 | 1.24 | 3.92 | 1.25 |
| TOM γ subunit | 17 | 3 | N ^a | <i>tomA4</i> | N ^a | 4.68 | 1.71 | 5.10 | 1.66 | 9.07 | 1.91 |
| TOM reductase | 6 | 3 | N ^a | <i>tomA5</i> | N ^a | 3.30 | 2.46 | 2.35 | 2.37 | 2.64 | 2.29 |
| γ-glutamylcysteine synthetase (GSHI* mutant) | 26 | 7 | b2688 | <i>gshA</i> | b2688 | 0.89 | 1.19 | 0.96 | 1.21 | 8.65 | 1.40 |
| 30S ribosomal subunit protein S13 | 40 | 5 | 16131177 | <i>rpsM</i> | b3298 | 2.19 | 1.15 | 0.85 | 1.06 | 1.99 | 1.21 |
| 30S ribosomal subunit protein S16 | 6 | 3 | 16130530 | <i>rpsP</i> | b2609 | 1.98 | 2.33 | 1.02 | 1.58 | 2.63 | 2.61 |
| 30S ribosomal subunit protein S3 | 47 | 8 | 16131193 | <i>rpsC</i> | b3314 | 2.28 | 1.21 | 1.26 | 1.08 | 1.73 | 1.34 |
| 50S ribosomal subunit protein L19 | 24 | 5 | 16130527 | <i>rplS</i> | b2606 | 2.79 | 1.19 | 1.30 | 1.16 | 2.54 | 1.35 |
| 50S ribosomal subunit protein L20, also post-translational autoregulator | 6 | 2 | 16129672 | <i>rplT</i> | b1716 | 3.65 | 1.37 | 1.45 | 1.18 | 2.73 | 2.43 |
| 50S ribosomal subunit protein L30 | 11 | 2 | 16131181 | <i>rpmD</i> | b3302 | 1.51 | 1.25 | 1.09 | 1.51 | 1.83 | 1.18 |
| 50S ribosomal subunit protein L32 | 8 | 2 | 16129052 | <i>rpmF</i> | b1089 | 2.79 | 1.20 | 3.32 | 2.10 | 1.28 | 1.16 |
| 50S ribosomal subunit protein L33 ^e | 7 | 1 | 16131507 | <i>rpmG</i> | b2636 | 1.55 | 1.14 | 1.65 | 1.27 | 2.58 | 1.46 |
| 50S ribosomal subunit protein L4, regulates expression of S10 operon | 40 | 6 | 16131198 | <i>rplD</i> | b3319 | 2.10 | 1.43 | 1.30 | 1.47 | 1.39 | 1.39 |
| cysteine synthase A | 24 | 8 | 16130340 | <i>cysK</i> | b2414 | 0.32 | 1.18 | 0.37 | 1.16 | 2.21 | 1.35 |
| sulfite reductase, α subunit | 2 | 2 | 16130670 | <i>cysI</i> | b2763 | 0.39 | 2.27 | 0.48 | 2.24 | 0.91 | 6.04 |
| cysteine desulfurase | 17 | 6 | 49176235 | <i>iscS</i> | b2530 | 1.22 | 1.19 | 1.23 | 1.18 | 1.91 | 1.30 |
| aminomethyltransferase of glycine cleavage system ^e | 1 | 1 | 16130807 | <i>gcvT</i> | b2905 | 0.18 | * | 0.16 | * | 0.47 | * |
| Tryptophanase | 120 | 18 | 49176396 | <i>tnaA</i> | b3708 | 0.19 | 1.11 | 0.15 | 1.12 | 0.13 | 1.15 |
| Succinate dehydrogenase, Fe-S protein | 8 | 2 | 16128699 | <i>sdhB</i> | b0724 | 0.67 | 1.22 | 0.77 | 1.31 | 0.51 | 1.35 |
| malate dehydrogenase | 37 | 7 | 16131126 | <i>mdh</i> | b3236 | 0.35 | 1.20 | 0.46 | 1.15 | 0.40 | 1.19 |
| phosphoenolpyruvate carboxykinase | 11 | 6 | 16131280 | <i>pckA</i> | b3403 | 0.47 | 1.51 | 0.59 | 1.48 | 0.43 | 1.62 |
| global regulator, starvation conditions | 15 | 3 | 16128780 | <i>dps</i> | b0812 | 1.45 | 1.19 | 1.84 | 1.29 | 1.85 | 1.21 |
| acetate kinase | 5 | 3 | 16130231 | <i>ackA</i> | b2296 | 1.88 | 1.51 | 1.13 | 3.41 | 3.78 | 3.41 |
| L-lactate dehydrogenase | 3 | 2 | 16131476 | <i>lldD</i> | b3605 | 1.47 | 1.54 | 1.55 | 1.22 | 1.63 | 1.47 |
| acetyl-CoA carboxylase (biotin carboxylase subunit) | 3 | 2 | 16131144 | <i>accC</i> | b3256 | 0.69 | 1.61 | 0.94 | 1.44 | 0.38 | 2.55 |
| malonyl-CoA-[acyl-carrier-protein] transacylase ^e | 2 | 1 | 16129055 | <i>fabD</i> | b1092 | 0.46 | 7.73 | 0.60 | 1.72 | 0.75 | 3.95 |
| Glycine tRNA synthetase, β subunit | 15 | 6 | 16131430 | <i>glyS</i> | b3559 | 1.32 | 1.31 | 1.28 | 1.17 | 1.73 | 1.63 |
| alkyl hydroperoxide reductase subunit | 21 | 4 | 16128589 | <i>ahpF</i> | b0606 | 4.06 | 1.43 | 3.07 | 1.13 | 1.90 | 1.22 |
| aminoacyl-histidine dipeptidase (peptidase D) | 5 | 3 | 16128223 | <i>pepD</i> | b0237 | 0.37 | 1.67 | 0.71 | 1.26 | 0.81 | 1.22 |
| carbamoyl phosphate synthase, large subunit | 3 | 3 | 16128027 | <i>carB</i> | b0033 | 1.41 | 2.88 | 1.02 | 2.21 | 1.26 | 2.64 |
| catalase, hydroperoxidase HPI(I) | 11 | 4 | 16131780 | <i>katG</i> | b3942 | 1.79 | 1.50 | 1.24 | 1.54 | 1.82 | 1.44 |
| chaperone Hsp90, heat shock protein C 62.5 | 46 | 14 | 16128457 | <i>htpG</i> | b0473 | 1.34 | 1.15 | 1.71 | 1.11 | 1.82 | 1.34 |
| DNA-bending protein with chaperone activity | 2 | 2 | 16130583 | <i>stpA</i> | b2669 | 1.00 | 1.94 | 1.25 | 2.30 | 1.70 | 1.89 |
| fructose-bisphosphate aldolase, class II | 20 | 4 | 16130826 | <i>fbpA</i> | b2925 | 0.55 | 1.27 | 0.70 | 1.12 | 1.15 | 1.28 |
| glycerophosphodiester phosphodiesterase, periplasmic | 10 | 6 | 16130174 | <i>glpQ</i> | b2239 | 0.46 | 1.75 | 0.55 | 1.31 | 0.49 | 1.83 |
| inorganic pyrophosphatase | 8 | 3 | 16132048 | <i>ppa</i> | b4226 | 1.04 | 1.42 | 1.44 | 1.16 | 0.41 | 2.87 |
| membrane-bound ATP synthase, delta-subunit | 7 | 2 | 16131603 | <i>atpH</i> | b3735 | 0.49 | 1.35 | 0.49 | 1.29 | 0.66 | 1.22 |
| NADH dehydrogenase I chain I | 9 | 3 | 16130216 | <i>nuoI</i> | b2281 | 0.68 | 1.20 | 0.83 | 1.21 | 0.36 | 1.40 |
| nucleoside diphosphate kinase | 7 | 2 | 16130443 | <i>ndk</i> | b2518 | 0.52 | 1.30 | 0.60 | 1.27 | 0.36 | 1.48 |
| oligopeptide transport protein (ABC superfamily) | 10 | 5 | 16129204 | <i>oppA</i> | b1243 | 0.41 | 1.16 | 0.79 | 1.25 | 0.64 | 1.55 |
| periplasmic glucans biosynthesis protein | 4 | 3 | 16129011 | <i>mdoG</i> | b1048 | 0.94 | 2.16 | 1.40 | 1.57 | 0.83 | 4.26 |
| periplasmic chaperone for outer membrane proteins ^e | 5 | 1 | 16128171 | <i>hlpA</i> | b0178 | 2.45 | 1.38 | 1.09 | 1.43 | 6.69 | 1.38 |
| serine hydroxymethyltransferase | 11 | 4 | 16130476 | <i>glyA</i> | b2551 | 0.28 | 1.42 | 0.45 | 1.34 | 0.45 | 2.00 |
| soluble pyridine nucleotide transhydrogenase | 3 | 2 | 16131800 | <i>udhA</i> | b3962 | 0.72 | 1.54 | 0.97 | 1.51 | 0.65 | 2.03 |
| Superoxide dismutase, iron | 3 | 2 | 16129614 | <i>sodB</i> | b1656 | 0.52 | 2.74 | 0.36 | 1.54 | 0.83 | 2.93 |
| threonine 3-dehydrogenase, NAD(P)-binding | 7 | 3 | 16131487 | <i>tdh</i> | b3616 | 0.67 | 1.39 | 0.47 | 1.55 | 0.99 | 1.46 |
| triosephosphate isomerase | 3 | 2 | 16131757 | <i>tpiA</i> | b3919 | 0.58 | 2.64 | 0.67 | 1.78 | 0.91 | 3.08 |
| uridine phosphorylase | 9 | 3 | 16131680 | <i>udp</i> | b3831 | 1.54 | 1.33 | 1.40 | 1.21 | 2.14 | 1.39 |

^a N: no corresponding number or synonym in *E. coli* K12 complete genome since proteins are cloned from *B. cepacia* G4. ^b Ratio: ratio of expression level in strain TG1/pBS(Kan)-TOM-Green/pMMB277- vs TG1/pBS(Kan)-/pMMB277-. ^c Ratio: ratio of expression level in strain TG1/pBS(Kan)-TOM-Green/pMMB277-IsoILR1 vs TG1/pBS(Kan)-/pMMB277-. ^d Ratio: ratio of expression level in strain TG1/pBS(Kan)-TOM-Green/pMMB277-IsoILR1-GSHI* vs TG1/pBS(Kan)-/pMMB277-. ^e De novo sequencing and manual checking done.

for the synthesis of cysteine and glycine (glutathione consists of cysteine, glutamate, and glycine) (Figure 1). Expression of γ-glutamylcysteine synthetase in TG1/TOM-Green/IsoILR1/GSHI* caused a 5.9–7-fold-induction of cysteine synthase A (*O*-acetylserine sulfhydrylase A, encoded by *cysK*), the enzyme which synthesizes cysteine and acetate from *O*-acetyl-L-serine

and H₂S (Figure 1),¹⁰ compared to the strains with either TOM-Green or TOM-Green/IsoILR1. Increasing cysteine, the substrate of γ-glutamylcysteine synthetase, should allow for greater glutathione synthesis and greater *cis*-DCE degradation due to the active glutathione *S*-transferase (GST) (Figure 1). Note that 9-fold more intracellular glutathione was measured after adding

Table 3. Relative Protein Expression of *E. coli* TG1 Cells Expressing TOM-Green/EchA F108L/I219L/C248I Relative to TOM-Green/Wild-Type EchA

| Protein Name | ID number | Gene | Synonym | Total > 70% | Distinct > 70% | Ratio ^a | EF ^a |
|---|----------------|-------------|----------------|-------------|----------------|--------------------|-----------------|
| EchA | N ^b | <i>echA</i> | N ^b | 86 | 6 | 2.14 | 1.31 |
| protein chain elongation factor EF-Ts | 16128163 | <i>tsf</i> | b0170 | 25 | 6 | 0.447 | 1.17 |
| 50S ribosomal subunit protein L7/L12 | 16131816 | <i>rplL</i> | b3986 | 7 | 6 | 0.591 | 1.18 |
| cysteine synthase A, O-acetylserine sulfhydrylase A | 16130340 | <i>cysK</i> | b2414 | 4 | 3 | 0.504 | 1.69 |
| Glycerophosphodiester phosphodiesterase | 16130174 | <i>glpQ</i> | b2239 | 31 | 5 | 0.499 | 1.13 |
| 50S ribosomal subunit protein L32 | 16129052 | <i>rpmF</i> | b1089 | 4 | 1 | 1.962 | 2.73 |
| 50S ribosomal subunit protein L29 | 16131191 | <i>rpmC</i> | b3312 | 21 | 1 | 0.503 | 1.07 |
| Iron superoxide dismutase | 16129614 | <i>sodB</i> | b1656 | 10 | 2 | 0.601 | 1.10 |

^a Ratio of expression level in strains TG1/TOM-Green/EchA-F108L/I219L/C248I vs TG1/TOM-Green/ EchA-wild-type. ^b No ID number or synonym since protein is from *A. radiobacter* AD1, not *E. coli*.

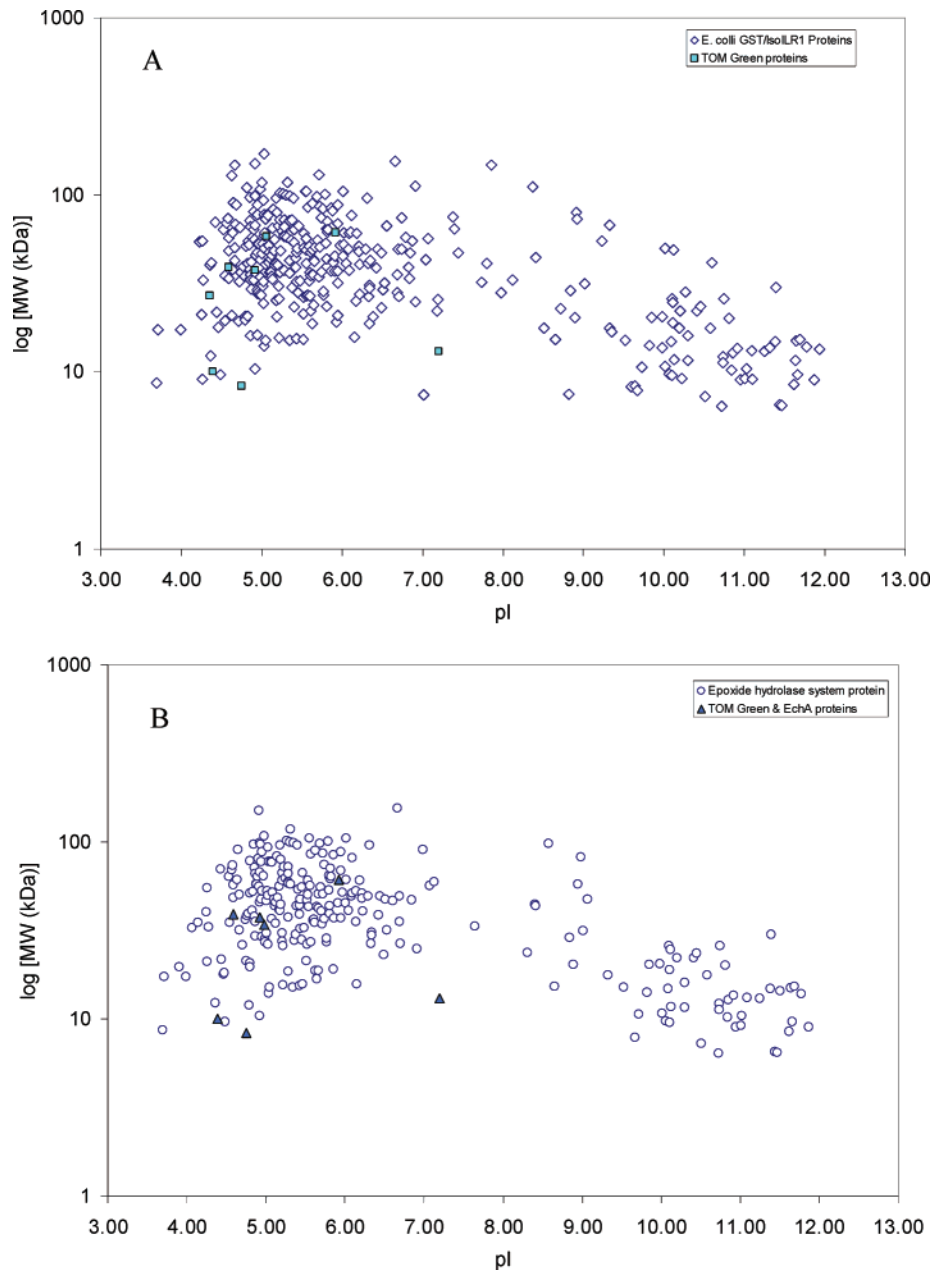


Figure 2. Protein identification and overall proteome coverage across pI and MW range. (A) *E. coli* TOM glutathione S-transferase system: \diamond denotes wild-type proteins identified in *E. coli*; \blacksquare denotes TOM-Green and GSH/IsoILR1-related proteins identified. (B) *E. coli* epoxide hydrolase system: \circ denotes wild-type proteins identified; \blacktriangle denotes TOM-Green and EchA-related proteins identified. GSHT^{*}; hence, the net result is that more glutathione is synthesized. Moreover, the expression level of two other proteins involved in the glutathione synthesis pathway was also changed significantly in all three strains with TOM-Green

(Figure 1). Aminomethyltransferase (encoded by *gcvT*) and serine hydroxymethyltransferase (encoded by *glyA*) were repressed 2–6-fold more in the strains with TOM-Green compared to the strain without TOM-Green (Table 2). Although the peptide identification evidence for the down-regulation of aminomethyltransferase has a doubtful statistical basis, similar repression of the well-identified/quantified (4 distinct peptides, 11 replicates; Table 2) serine hydroxymethyltransferase that diverges to a similar intermediate glycine was indicative for validating down-regulation. Aminomethyltransferase initiates the conversion of glycine to CO₂, NH₃, and methylene,¹¹ and serine hydroxymethyltransferase catalyzes the reversible interconversion of serine and glycine with tetrahydrofolate¹² (Figure 1). Down-regulation of these proteins may allow greater glycine for glutathione synthesis.

As another interesting enzyme directly related with *cis*-DCE degradation, tryptophanase (encoded by *tnaA*, primarily degrades L-tryptophan to indole, pyruvate, and ammonia¹³) was repressed 5–8-fold in the TOM-Green-containing strains compared to the strain without TOM-Green (Table 2). Since TOM-Green catalyzes indole oxidation¹⁴ as well as that of *cis*-DCE, down-regulation of tryptophanase expression may allow more *cis*-DCE degradation in the TOM-Green systems.

Beyond the proteins involved directly in *cis*-DCE detoxification, the expression levels of enzymes related to carbon flux, fatty acid synthesis, and oxidative stress proteins were altered due to the introduction of TOM-Green, IsoILR1, or GS^{HI}* (Table 2). Adding TOM-Green up-regulated the expression levels of ribosomal protein subunits, stress response proteins, a global regulator of starvation conditions, and enzymes involved in pyruvate metabolism. In contrast, enzymes related with the TCA cycle and fatty acid synthesis were down-regulated. Specifically, expression of TOM-Green alone caused a 2–3.6-fold up-regulation of the expression of seven ribosomal subunits (out of a total of 47 identified ribosomal 30S and 50S subunit proteins) including the 30S ribosomal subunit proteins S3 (encoded by *rpsC*); S13 (encoded by *rpsM*); S16 (encoded by *rpsP*); and the 50S ribosomal subunit proteins L19 (encoded by *rplS*), L20 (encoded by *rplT*), and L32 (encoded by *rpmF*) compared to the strain without TOM-Green (Table 2). Upon expression of TOM-Green/IsoILR1, the 50S ribosomal subunit protein L32 was increased 3-fold relative to the strain without TOM-Green (Table 2). For the strain containing TOM-Green/IsoILR/GS^{HI}*, the expression level of the 30S ribosomal subunit proteins S3, S13, S16, and the 50S ribosomal subunit proteins L19, L20, L30 (encoded by *rpmD*), and L33 were induced about 2-fold compared to the strain without TOM-Green (Table 2). Although the exact roles of all individual ribosomal proteins were not fully characterized, it has been reported that several ribosomal proteins are modulated in response to reactive oxygen species, cadmium, and low temperature.^{15–17} For example, *E. coli* induces transcription of S3, S10, S19, L2, L4, L6, L10, L23, and L29 upon addition of the superoxide-generating agent paraquat.¹⁶ Unlike *cis*-DCE degradation, the addition of cadmium represses transcription of L2, L3, L4, S3, S5, and S16 but induces transcription of L9 and L20 in *E. coli*.¹⁵ Therefore, the results here confirm that the ribosomal proteins S3 (an inducer of antiapoptotic proteins),¹⁸ S16 (an essential element for 30S assembly),¹⁹ and L20 (involved in negative autogenous regulation)²⁰ probably play important roles in the *E. coli* stress response. Also, these data suggest that the response to *cis*-DCE degradation in *E. coli* is similar to the response to reactive oxygen species. Furthermore, the up-

regulation of the ribosomal subunit proteins may be a general response to the metabolic engineering, in that the addition of the nine genes here may result in translational limitations.²¹

Overexpression of TOM-Green in the engineered strains led to the production of toxic *cis*-DCE epoxide and glyoxal; as a result, *dps*, which encodes the global regulator of starvation conditions and whose protein protects DNA from oxidative or nutritional stresses in *E. coli*,²² was induced 1.5–1.8-fold in the strains with TOM-Green compared to the strain without TOM-Green (Table 2). Up-regulation of this protein probably plays an important role for enhancing the ability of the cells to tolerate intermediates like *cis*-DCE epoxide and glyoxal.

Moreover, the proteomic data also shows that the expression level of proteins involved in catalysis of hydroperoxides has been changed in all three strains with TOM-Green. The alkyl hydroperoxide reductase subunit [FAD/NAD(P)-binding, encoded by *ahpF*]²³ was up-regulated 2–4-fold in all three strains with TOM-Green, and catalase [hydroperoxidase HPI (I), encoded by *katG*]²⁴ was up-regulated about 1.8-fold in the strains with either TOM-Green/IsoILR or TOM-Green/IsoILR/GS^{HI}* compared to the strain without TOM-Green (Table 2). In contrast, the strains with either TOM-Green or TOM-Green/IsoILR1 down-regulated the expression level of iron superoxide dismutase (encoded by *sodB*), which catalyzes the conversion of superoxide radicals to hydrogen peroxide and oxygen²⁵ (Table 2). These results also support the theory that the stress response mechanism that is incurred during aerobic *cis*-DCE degradation in *E. coli* is close to the defense mechanism for reactive oxygen species.

When TOM-Green was introduced, the pyruvate metabolism was also affected (Figure 3). In the strain containing TOM-Green/IsoILR1/GS^{HI}*, the expression level of acetate kinase (encoded by *ackA*) was induced around 3-fold compared to the strain without TOM-Green/IsoILR1/GS^{HI}* (Table 2). Also, the expression level of L-lactate dehydrogenase (encoded by *lldD*) was up-regulated in all three strains with TOM-Green (Figure 3). Lactate dehydrogenase converts lactate to pyruvate in mixed acid fermentations and glucose heterofermentation,^{26,27} and acetate kinase catalyzes the reversible conversion of acetate and acetyl phosphate²⁸ (Figure 3). The induction of these enzymes results probably in an increase in the intracellular level of acetyl phosphate or acetyl-CoA (Figure 3), suggesting that the metabolic pathways for energy transfer and carbon source flux were altered in the best-engineered strain for *cis*-DCE detoxification.

In contrast, the introduction of TOM-Green appears to influence carbon flux by repressing enzymes for the tricarboxylic acid cycle (TCA cycle), gluconeogenesis, and fatty acid synthesis (Figure 3). For example, malate dehydrogenase (encoded by *mdh*), the enzyme that catalyzes the interconversion of malate and oxaloacetate in the TCA cycle,²⁹ was repressed 2-fold in the three strains with TOM-Green compared to the strain without TOM-Green (Table 2, Figure 3). Also, the expression of succinate dehydrogenase (encoded by *sdhB*) was repressed about 2-fold in the strain with TOM-Green/IsoILR1/GS^{HI}* compared to the strain without TOM-Green (Table 2, Figure 3). Hence, the TCA cycle appears to be affected by the addition of TOM-Green, IsoILR1, and GS^{HI}*. In addition, enzymes involved in gluconeogenesis, for example, phosphoenolpyruvate carboxykinase (encoded by *pckA*), the enzyme that catalyzes the conversion of oxaloacetate to phosphoenolpyruvate and carbon dioxide,³⁰ were repressed 2-fold in

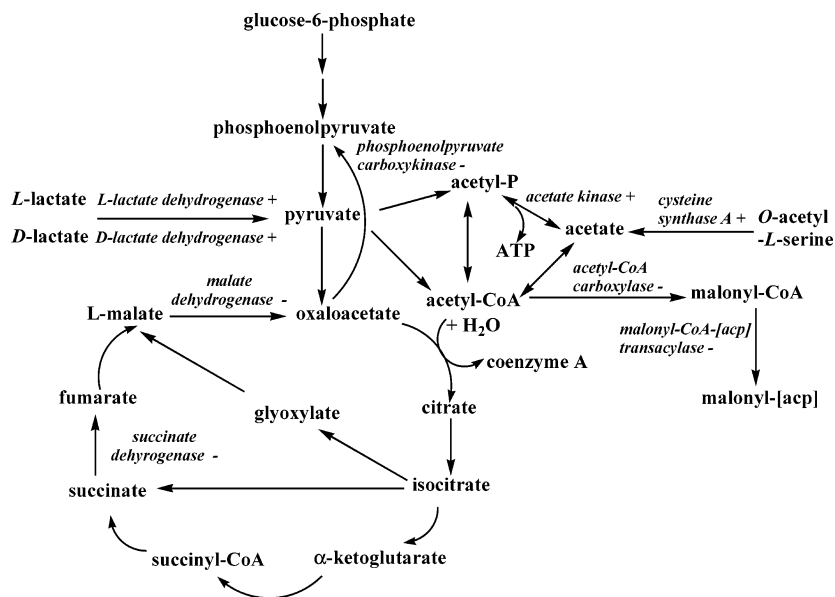


Figure 3. Impact of metabolic engineering on the gluconeogenesis, glyoxylate bypass, and TCA pathways for *cis*-DCE detoxification by TG1/TOM-Green/IsoILR1/GSHI* and TG1/TOM-Green/EchA-F108L/I219L/C248I. The "+" indicates overexpression, while "-" indicates repression of the proteins. ATP is adenosine triphosphate, Acetyl-P is acetyl phosphate, and [acp] is acyl-carrier-protein.

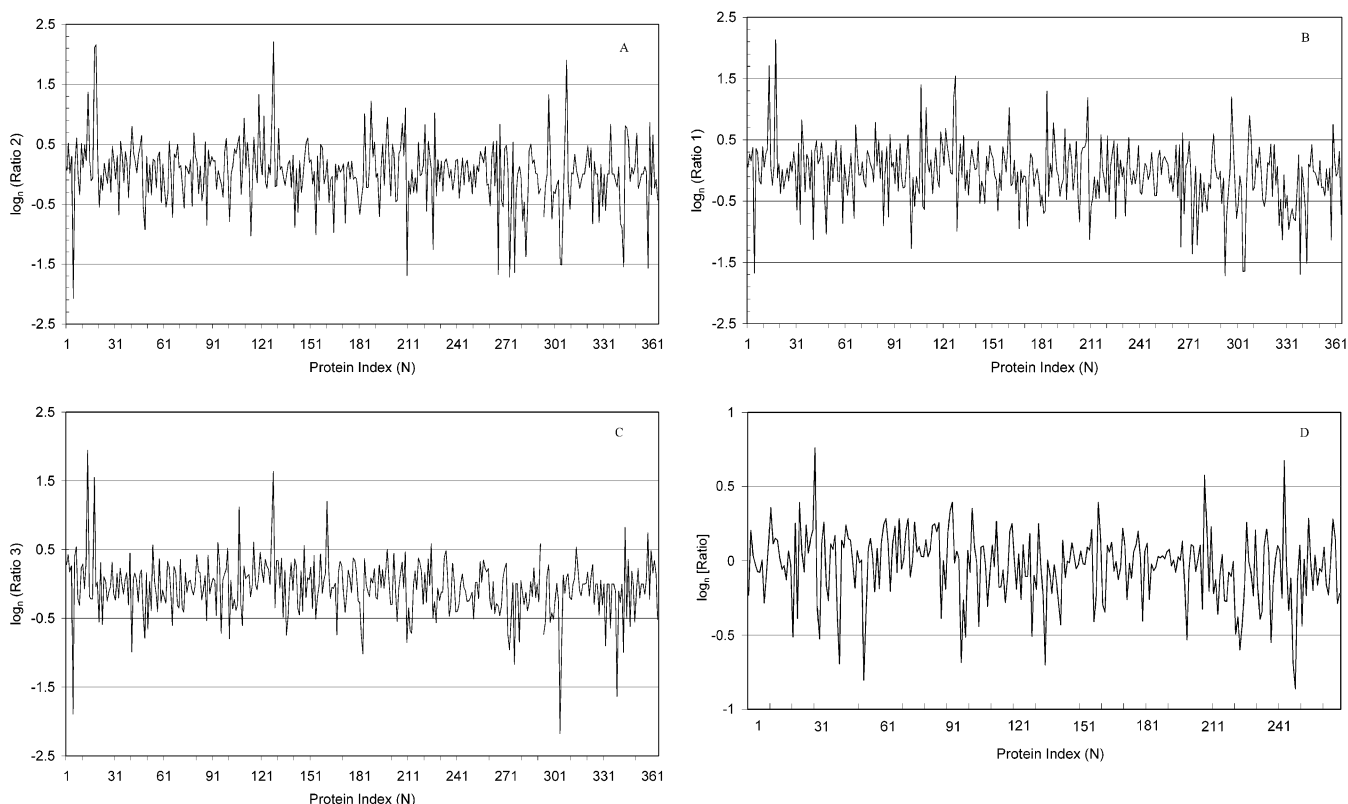


Figure 4. Protein expression ratio comparison across protein index. (A) Protein expression ratio for TG1/pBS(Kan)-TOM-Green/pMMB277-IsoILR1-GSHI* against TG1/pBS(Kan)-pMMB277; (B) protein expressions ratio for TG1/pBS(Kan)-TOM-Green/pMMB277 against TG1/pBS(Kan)-pMMB277; (C) protein expressions ratio for TG1/pBS(Kan)-TOM-Green/pMMB277-IsoILR1 against TG1/pBS(Kan)-pMMB277; (D) epoxide hydrolase system: protein expression ratio for TG1/TOM-Green/EchA-F108L/I219L/C248I against TG1/TOM-Green/EchA-wild-type. All plots are presented with a logarithmic scale. Peaks and readings that are nonzero denote differently expressed proteins.

the strains upon adding TOM-Green (Table 2, Figure 3). This probably resulted in reduced concentrations of phosphoenopyruvate and, subsequently, reduced glucose-6-phosphate concentrations in the engineered strains. This suggests carbon flux was re-directed from glucose.

Two enzymes of fatty acid synthesis, malonyl-CoA-[acyl-carrier-protein] transacylase (encoded by *fabD*)³¹ and acetyl-CoA carboxylase (biotin carboxylase subunit encoded by *accC*)³² were reduced approximately 2-fold by adding TOM-Green (Table 2), which indicates fatty acid may be significantly altered.

Acetyl-CoA carboxylase consists of a biotin carboxylase, a carboxyltransferase for carboxylation, and a biotin carboxyl carrier protein for carrying biotin; this enzyme catalyzes the first step in fatty acid synthesis to form malonyl-CoA³² (Figure 3). Although the statistical basis for the identification of malonyl-CoA transacylase was not calculated due to the lack of multiple high-scoring peptides (Table 2), the presence of acetyl-CoA carboxylase upstream of the metabolic pathway that also experienced similar down-regulation with better statistical basis provided cross-referencing evidence to the likely reliability of this quantification. The corresponding spectrum was also manually de novo-sequenced and checked for any misinterpretation by the ProQuant software v1.1 (Applied Biosystems, MDS Sciex).

In addition, the expression level of many proteins was changed, although their exact roles in the *cis*-DCE degradation are unclear (Table 2). All three strains with TOM-Green distinctively up-regulated glycine tRNA synthetase (β subunit, encoded by *glyS*), chaperone Hsp90 (heat shock protein C 62.5, encoded by *htpG*), the periplasmic molecular chaperone for outer membrane proteins (encoded by *hlpA*), and uridine phosphorylase (encoded by *udp*), while these strains significantly down-regulated glycerophosphodiester phosphodiesterase (periplasmic, encoded by *glpQ*) and membrane-bound ATP synthase (F1 sector, δ -subunit, encoded by *atpH*).

Epoxide Hydrolase System Proteome. Out of the 268 proteins identified from both *E. coli* TG1 strains harboring TOM-Green/EchA-wild-type and TOM-Green/EchA F108L/I219L/C248I (Figure 2), the expression level of 8 proteins changed significantly (Table 3) due to the metabolic engineering which produced the first active epoxide hydrolase for chlorinated ethenes.³ Since we compared the evolved EchA versus the wild-type EchA enzyme, less proteins changed in the epoxide hydrolase system compared to adding extra enzymes in the glutathione *S*-transferase system. Both EchA and the 50S ribosomal subunit protein L32 in the strain with the evolved EchA F108L/I219L/C248I were expressed about 2-fold greater than the strain which contained wild-type EchA (Table 3). Intriguingly, the expression of L32 was up-regulated in the strain with TOM-Green/EchA F108L/I219L/C248I as well as in all three TOM-Green systems. *rpmF* encoding ribosomal protein L32 is upstream of *plsX* (unknown function) and the *fab* cluster (encoding key fatty acid synthetic enzymes).³³ Cotranscription of *rpmF* and *plsX* plays an important role in the coordinate regulation of ribosomes and cell membrane synthesis,^{33,34} so perhaps L32 was expressed along with these other loci. However, other proteins such as protein chain elongation factor EF-Ts, the 50S ribosomal subunit proteins L7/L12/L29, and iron superoxide dismutase in the EchA triple mutant system were decreased about 2-fold compared to the strain with wild-type EchA (Table 3). It is interesting that the protein level of superoxide dismutase was down-regulated in the EchA triple mutant as well as in the TOM-Green system compared to their respective controls. The expression level of cysteine synthase A and glycerophosphodiester phosphodiesterase in the strain with EchA-F108L/I219L/C248I were also decreased 2-fold compared to the strain with wild-type EchA. We note that no extra cysteine is needed for the reaction carried out by EchA toward *cis*-DCE epoxide (water takes the place of glutathione) (Figure 1); hence, in the strain with EchA F108L/I219L/C248I, the metabolic pathway of the GST/GSHI* system was repressed 2-fold with a lower expression level of cysteine synthase A compared with the strain containing the wild-type

EchA. These results also suggest lower expression of these enzymes in the strain containing EchA F108L/I219L/C248I was useful for greater *cis*-DCE degradation.

Discussion

We show clearly in this work that the physiology of *E. coli* cells is altered when contacted with 1 mM *cis*-DCE by the introduction of TOM-Green, IsoILR1, and GSHI* or by engineering EchA from wild-type to the F108L/I219L/C248I variant so that the epoxide hydrolase effectively detoxifies the chlorinated epoxide formed from TOM-Green oxidation of *cis*-DCE. We used a multiplexed peptide quantification technique (iTRAQ)⁶ to identify and quantify the protein expression changes between control cells and engineered *E. coli* cells. The proteomic data clearly show the beneficial changes of the expression level of important enzymes involved in the metabolic pathway of *cis*-DCE degradation (Figure 1). The data also show that the TCA cycle, the fatty acid formation pathway, and acetyl-CoA pathway were probably influenced by the introduction of TOM-Green, IsoILR1, and GSHI* (Figure 3). Moreover, this study elucidates a number of interesting stress-activated proteins that were regulated during aerobic degradation of *cis*-DCE.

As expected, the expression levels of enzymes involved directly in *cis*-DCE detoxification pathway were up-regulated in the glutathione *S*-transferase system by the introduction of TOM-Green, IsoILR1, and GSHI* (Figure 1). Hence, to enhance *cis*-DCE detoxification, the cell overexpresses cysteine synthase A and represses aminomethyltransferase and serine hydroxymethyltransferase to achieve higher concentrations of intracellular glutathione. Although glutathione synthetase (encoded by *gshB*) (Figure 1) was not identified in this study, overexpression of glutathione synthetase which produces glutathione or addition of exogenous glutathione may further enhance *cis*-DCE detoxification in the *E. coli* strain with TOM-Green/IsoILR1/GSHI*. Use of a tryptophanase (*tnaA*) knockout strain that forms less indole may also help *cis*-DCE oxidation because indole serves as a competitive substrate for TOM-Green.

The engineered strains in both systems produce toxic intermediates, such as *cis*-DCE epoxide and glyoxal (Figure 1). Although *cis*-DCE epoxide degradation has been addressed with our engineered cells, the toxicity of glyoxal remains. This may be addressed by identifying or evolving an enzyme that can convert glyoxal into a product capable of being utilized in central metabolism cycles.⁴ For example, overexpression of glyoxalase I and glyoxalase II that catalyze the conversion of methylglyoxal into D-lactate³⁵ or overexpression of aldehyde dehydrogenase that could theoretically catalyze glyoxal into glyoxylate (Figure 3) may be beneficial for channeling glyoxal into a central metabolic cycle.³⁶

Other metabolic pathways such as the TCA cycle, gluconeogenesis, the acetyl-CoA pathway, and fatty acid synthesis were affected by the metabolic engineering (Figure 3). As the key compound related to gluconeogenesis and the TCA cycle, L-malate plays an important role in carbon flux in *E. coli* (Figure 3).^{26,37} In the TCA cycle, succinate is converted to fumarate by succinate dehydrogenase and is sequentially catalyzed to malate by fumarase.²⁶ Repression of succinate dehydrogenase (an Fe-S protein) in the TCA cycle should lead to less L-malate generated from fumarate (Figure 3).

Acetyl-CoA is a precursor of many different molecules including citrate, lipids, and fermentation end products²⁶ (Figure 3). The accumulation of acetyl-CoA in the strain containing TOM-Green/IsoILR1/GSHI* was probably from (i)

2-fold depression of fatty acid synthesis; (ii) 2-fold induction of cysteine synthase A which produces acetate and cysteine formed from *O*-acetyl-L-serine;³⁸ (iii) 3.8-fold induction of acetate kinase, which converts acetyl phosphate to acetate in the mixed acid fermentation;²⁶ and (iv) 1.7-fold up-regulation of a lactate dehydrogenase (Figure 3). Since some of the components of the TCA cycle and fatty acid synthesis pathways were down-regulated in the engineered cells compared to the control cells, the strains with TOM-Green might try to use acetyl-CoA to produce ATP via acetyl phosphate during *cis*-DCE degradation (Figure 3). This speculation may partially explain the higher cell viability with the strain that contains TOM-Green/IsoILR1/GSHI* (Table 2).

Over 20 years, a variety of approaches using two-dimensional electrophoresis and DNA microarrays has led to the identification of various important reactive oxygen-activated genes including *katG*, *ahpF*, *dps*, *gorA*, *oxyS*, *grxA*, *fur*, *trxC*, *dsbG*, *fhuF*, and *flu*.³⁹ In this study, a quantitative shotgun approach identified that the expression levels of three proteins, catalase (encoded by *katG*), alkyl hydroperoxide reductase subunit (encoded by *ahpF*), and a global regulator (encoded by *dps*), were up-regulated (1.5–4.0-fold) in all three *E. coli* strains with TOM-Green compared to the strain without TOM-Green (Table 2). Also, we could detect that the expression level of iron superoxide dismutase (encoded by *sodB*)²⁵ was influenced; this protein is another interesting reactive oxygen-activated protein.²⁵ Moreover, a total of nine interesting ribosomal proteins including S3, S16, L20, and L32 were significantly up-regulated (Table 2) during aerobic *cis*-DCE degradation which may indicate they, like other ribosomal proteins, are playing a significant role in oxygen-related stress response as a result of converting *cis*-DCE to *cis*-DCE epoxide and glyoxal or that there is a translational limitation.²¹

In this study, the proteomic data provide important insights into the metabolic and physiological changes that occur upon *cis*-DCE degradation by engineered *E. coli* strains. Since the number of identified proteins in this quantitative proteomic approach is less than the number of genes, a DNA microarray analysis may complement this proteomic approach.

Acknowledgment. This research was supported by the National Science Foundation (BES-0331416) and the United Kingdom's Engineering and Physical Sciences Research Council (EPSRC) (GR/S84347/01). P.C.W. also thanks the EPSRC for provision of an Advanced Research Fellowship (GR/A11311/01).

Supporting Information Available: Expression ratios, *P*-values, and error factors for proteins identified from the glutathione *S*-transferase and the epoxide hydrolase systems; false-positive identification lists; and ion chromatograms. This material is available free of charge via the Internet at <http://pubs.acs.org>.

References

- (1) Ryoo, D.; Shim, H.; Canada, K.; Barbieri, P.; Wood, T. K. *Nat. Biotechnol.* **2000**, *18*, 775–778.
- (2) McCarty, P. L. *Science* **1997**, *276*, 1521–1522.
- (3) Rui, L.; Cao, L.; Chen, W.; Reardon, K. F.; Wood, T. K. *J. Biol. Chem.* **2004**, *279*, 46810–46817.

- (4) Rui, L.; Kwon, Y. M.; Reardon, K. F.; Wood, T. K. *Environ. Microbiol.* **2004**, *6*, 491–500.
- (5) Canada, K. A.; Iwashita, S.; Shim, H.; Wood, T. K. *J. Bacteriol.* **2002**, *184*, 344–349.
- (6) Ross, P. L.; Huang, Y. N.; Marchese, J. N.; Williamson, B.; Parker, K.; Hattan, S.; Khainovski, N.; Pillai, S.; Dey, S.; Daniels, S.; Purkayastha, S.; Juhasz, P.; Martin, S.; Bartlet-Jones, M.; He, F.; Jacobson, A.; Pappin, D. J. *Mol. Cell. Proteomics* **2004**, *3*, 1154–1169.
- (7) Aggarwal, K.; Choe, L. H.; Lee, K. H. *Proteomics* **2005**, *5*, 2297–2308.
- (8) Sambrook, J.; Fritsch, E. F.; Maniatis, T. *Molecular Cloning: A Laboratory Manual*, 2nd ed.; Cold Spring Harbor Laboratory Press: Cold Spring Harbor, New York, 1989.
- (9) Chong, P. K.; Gan, C. S.; Pham, T. K.; Wright, P. C. *J. Proteome Res.* **2006**, published online Mar 25, <http://dx.doi.org/10.1021/pr060018u>.
- (10) Rabeh, W. M.; Cook, P. F. *J. Biol. Chem.* **2004**, *279*, 26803–26806.
- (11) Wonderling, L. D.; Urbanowski, M. L.; Stauffer, G. V. *Microbiology* **2000**, *146*, 2909–2918.
- (12) Schirch, V.; Szebenyi, D. M. *Curr. Opin. Chem. Biol.* **2005**, *9*, 482–487.
- (13) Gong, F.; Yanofsky, C. *J. Biol. Chem.* **2002**, *277*, 17095–17100.
- (14) Rui, L.; Reardon, K. F.; Wood, T. K. *Appl. Microbiol. Biotechnol.* **2005**, *66*, 422–429.
- (15) Wang, A.; Crowley, D. E. *J. Bacteriol.* **2005**, *187*, 3259–3266.
- (16) Pomposiello, P. J.; Bennik, M. H.; Demple, B. *J. Bacteriol.* **2001**, *183*, 3890–3902.
- (17) Sahara, T.; Goda, T.; Ohgiya, S. *J. Biol. Chem.* **2002**, *277*, 50015–50021.
- (18) Ruggero, D.; Pandolfi, P. P. *Nat. Rev. Cancer* **2003**, *3*, 179–192.
- (19) Persson, B. C.; Bylund, G. O.; Berg, D. E.; Wikstrom, P. M. *J. Bacteriol.* **1995**, *177*, 5554–5560.
- (20) Olsson, C. L.; Graffe, M.; Springer, M.; Hershey, J. W. *Mol. Gen. Genet.* **1996**, *250*, 705–714.
- (21) Wood, T. K.; Peretti, S. W. *Biotechnol. Bioeng.* **1990**, *36*, 865–878.
- (22) Zhao, G.; Ceci, P.; Ilari, A.; Giangiacomo, L.; Laue, T. M.; Chiancone, E.; Chasteen, N. D. *J. Biol. Chem.* **2002**, *277*, 27689–27696.
- (23) Bieger, B.; Essen, L. O. *J. Mol. Biol.* **2001**, *307*, 1–8.
- (24) Hillar, A.; Peters, B.; Pauls, R.; Loboda, A.; Zhang, H.; Mauk, A. G.; Loewen, P. C. *Biochemistry* **2000**, *39*, 5868–5875.
- (25) Kim, S. Y.; Nishioka, M.; Hayashi, S.; Honda, H.; Kobayashi, T.; Taya, M. *Appl. Environ. Microbiol.* **2005**, *71*, 2762–2765.
- (26) White, D. *The Physiology and Biochemistry of Prokaryotes*; Oxford University Press: New York, 2000.
- (27) Lu, Z.; Cabisco, E.; Obradors, N.; Tamarit, J.; Ros, J.; Aguilar, J.; Lin, E. C. *J. Biol. Chem.* **1998**, *273*, 8308–8316.
- (28) Fox, D. K.; Roseman, S. *J. Biol. Chem.* **1986**, *261*, 13487–13497.
- (29) Park, S.-J.; Cotter, P. A.; Gunsalus, R. P. *J. Bacteriol.* **1995**, *177*, 6652–6656.
- (30) Delbaere, L. T. J.; Sudom, A. M.; Prasad, L.; Leduc, Y.; Goldie, H. *Biochim. Biophys. Acta* **2004**, *1697*, 271–278.
- (31) Serre, L.; Verbree, E. C.; Dauter, Z.; Stuitje, A. R.; Derewenda, Z. S. *J. Biol. Chem.* **1995**, *270*, 12961–12964.
- (32) Li, S.-J.; Cronan, J. E., Jr. *J. Biol. Chem.* **1992**, *267*, 855–863.
- (33) Podkovyrov, S.; Larson, T. J. *FEBS Lett.* **1995**, *368*, 429–431.
- (34) Zhang, Y.; Cronan, J. E., Jr. *J. Bacteriol.* **1998**, *180*, 3295–3303.
- (35) Clugston, S. L.; Barnard, J. F.; Kinach, R.; Miedema, D.; Ruman, R.; Daub, E.; Honek, J. F. *Biochemistry* **1998**, *37*, 8754–8763.
- (36) van Hylckama Vlieg, J. E. T.; Janssen, D. B. *J. Biotechnol.* **2001**, *85*, 81–102.
- (37) Cronan, J. E., Jr.; LaPorte, D. In *Escherichia coli and Salmonella: Cellular and Molecular Biology*, 2nd ed.; Neidhardt, F. C., Ed.; ASM Press: Washington, DC, 1996; pp 206–216.
- (38) Kredich, N. M. In *Escherichia coli and Salmonella: Cellular and Molecular Biology*, 2nd ed.; Neidhardt, F. C., Ed.; ASM Press: Washington, DC, 1996; pp 514–527.
- (39) Zheng, M.; Wang, X.; Templeton, L. J.; Smulski, D. R.; LaRossa, R. A.; Storz, G. *J. Bacteriol.* **2001**, *183*, 4562–4570.

PR060008T